Coupled Systems Mechanics, *Vol. 4, No. 4 (2015) 317-336*
DOI: http://dx.doi.org/10.12989/csm.2015.4.4.317

2D Finite element analysis of rectangular water tank with separator wall using direct coupling

Kalyan Kumar Mandal* and Damodar Maity[a]

Department of Civil Engineering, Indian Institute Technology, Kharagpur, India

(Received May 26, 2015, Revised November 17, 2015, Accepted December 12, 2015)

Abstract. The present paper deals with the analysis of water tank with elastic separator wall. Both fluid and structure are discretized and modeled by eight node-elements. In the governing equations, pressure for the fluid domain and displacement for the separator wall are considered as nodal variables. A method namely, direct coupled for the analysis of water tank has been carried out in this study. In direct coupled approach, the solution of the fluid-structure system is accomplished by considering these as a single system. The hydrodynamic pressure on tank wall is presented for different lengths of tank. The results show that the magnitude of hydrodynamic pressure is quite large when the distances between the separator wall and tank wall are relatively closer and this is due to higher rotating tendency of fluid and the higher sloshed displacement at free surface.

Keywords: finite element; direct coupling; indirect coupling; sloshed displacement; elastic separator wall

1. Introduction

The interaction between an elastic structure and compressible fluid adjacent to it due to dynamic loading has become the subject of intensive investigation in recent years. An analytical solution of the wave equation to obtain the hydrodynamic pressure on the vertical face of the structures during earthquake presented by Chopra (1967) presented. Similar analytical solution for upstream face was evaluated by Chwang (1978). However, these analytical cannot account for the arbitrary geometry of the structure and this problem can be efficiently tackled with finite element technique. Finite element formulations based on displacement variables are usually chosen for the structure while the fluid is described by different variables such as displacement, pressure, velocity, velocity potential etc. The governing equations of fluid in terms of displacements are carried out by many researchers (Olson and Bathe 1983, Chen and Taylor 1990, Bermudez *et al*. 1995, Maity and Bhattacharyya 1997). In such formulation, the fluid elements can easily be coupled to the structural elements using standard finite element assembly procedures. But the degrees of freedom for fluid domain increase significantly. Bouaanani and Lu (2009) considered the velocity potential be the nodal variable for the analysis of reservoir adjacent to dams. Biswal *et al.* (2006) studied the sloshing of liquid on various shape of the container. The velocity potential is considered as

∗Corresponding author, Research Scholar, E-mail: kkma_iitkgp@yahoo.co.in
[a] Professor

http://www.techno-press.org/?journal=csm&subpage=7 ISSN: 2234-2184 (Print), 2234-2192 (Online)

independent variable in their finite element modeling. A similar study was conducted by Pal and Bhattacharyya (2013)

Tung (1979) studied the hydrodynamic pressure distribution on a rigid, submerged, cylindrical storage tank subjected to horizontal base excitation. The author considered fluid to be incompressible. Williams and Moubayed (1990) calculated hydrodynamic pressure on rigid tank walls due to horizontal and vertical excitations. The effects of a bottom-mounted rectangular block on the sloshing characteristics of the fluid in rectangular tanks were investigated by Chounand Yun (1996) using the linear water wave theory. The hydrodynamic pressure exerted on the tank wall was also calculated and the study showed the influence mounted block size and position. Consequent experimental study by Panigrahy *et al*. (2009) showed that the pressure exerted on the walls varies in a similar nature as that of the applied excitation. Barrios *et al*. (2007) studied the nonlinear sloshing response of cylindrical tanks. Hua *et al*. (2013) simulated fluid sloshing and sloshing induced hydrodynamic pressure on tank walls. Their study shows the influences of excitation frequency on hydrodynamic on rigid tank wall. However, all the above numerical simulations are carried out considering tank walls to be rigid. The deformations, stresses and hydrodynamic pressure will be more realistic if the elastic properties of tank walls and wall-fluid interaction are considered appropriately.

Many simplified approaches are available to deal fluid-structure interaction problem. Some of which, fluid-structure interaction is studied indirect approach, indirect iterative approach (Maity and Bhattacharyya 2003, Akkose *et al.* 2008, Onate *et al.* 2006, Singh *et al.* 1991, Lotf 2004, Antoniadis and Kanarachos 1998, Gogoi and Maity 2005, Pani and Bhattacharya 2003). In this method, the hydrodynamic pressure in fluid domain is first determined considering structure as rigid. The resulting pressure exerts forces on the adjacent structure. Due to this additional forces structure undergoes new displacement. The fluid domain is solved again with the calculated displacement to get the response of the elastic structures. The process is continued till a desired level of convergence in both pressures and displacements are achieved. However, the main disadvantages of this method are that the accuracy this analysis depends on the tolerance value and it requires more computational time and large computer storage as this analysis procedure is iterative in nature.

To compensate the inadequacies of this analyses procedure, an efficient direct finite element approach is developed. In this direct approach, structure and fluid are coupled and solved as a single system. In present study, a pressure-displacement based direct coupling approach is developed to obtain responses of water-separator wall system. A computer code in MATLAB environment has been developed to obtain hydrodynamic pressure, displacement and stresses on separator wall. The study is carried out for different tank dimensions against horizontal ground excitations.

2. Theoretical formulation

2.1 Theoretical formulation for wall

The equation of motion of a structure subjected to external forces can be written in standard finite element form as

$$\left[M_i\right]\left\{\ddot{u}_i\right\}+\left[C_i\right]\left\{\dot{u}_i\right\}+\left[K_i\right]\left\{u_i\right\}=\left\{F_{di}\right\} \tag{1}$$

Where, $\{\ddot{u}_i\}$, $\{\dot{u}_i\}$ and $\{u_i\}$ are nodal accelerations, velocities and displacements, $\{F_{di}\}$ is the nodal forces. Mass matrix, $[M_i]$ and stiffness $[K_i]$ may be expressed as follows.

$$[M_i] = \iiint\limits_V [N_w^T]\rho\,[N_w]\,dV \quad and \quad [K_i] = \iiint\limits_V [B^T][D]\,[B]\,dV \tag{2}$$

Where, *[N$_w$]* is shape function matrix, *[B]* is strain displacement matrix, *[D]* is strain displacement matrix and ρ is density of the wall. However, in present investigation, the tank walls have been discretised by two dimensional eight node rectangular elements and walls are assumed to behave linearly and are in a state of plane strain. The Rayleigh damping is considered as structural damping. Therefore, the damping matrix, $[C_i]$ can be expressed as

$$[C] = a'[M] + b'[K] \tag{3}$$

Here, a' and b' are called the proportional damping constants. The relationship between a', b' and the fraction of critical damping at a frequency ω is given by the following equation.

$$\xi' = \frac{1}{2}\left(a'\omega + \frac{b'}{\omega}\right) \tag{4}$$

Damping constants a' and b' are determined by choosing the fraction of critical damping ξ_1' and ξ_2' at two different frequencies ω_1 & ω_2 and solving simultaneously equations a' and b'. Thus

$$a' = \frac{2(\xi_2'\omega_2 - \xi_1'\omega_1)}{(\omega_2^2 - \omega_1^2)}$$
$$b' = \frac{2\omega_1\omega_2(\xi_2'\omega_1 - \xi_1'\omega_2)}{(\omega_2^2 - \omega_1^2)} \tag{5}$$

Usually, ω_1 is taken as the lowest natural frequency of the structure, and ω_2 is the highest frequency of interest in the loading or response. In the present study, the fraction of critical damping for both the frequencies are chosen as the same i.e. ξ_1' ’= ξ_2' ’= ξ'. Thus, above equation may be expressed as

$$a' = \frac{2\xi'}{(\omega_2 + \omega_1)}$$
$$b' = \frac{2\xi'\omega_1\omega_2}{(\omega_2 + \omega_1)} \tag{6}$$

2.2 Theoretical formulation for fluid

For a Newtonian fluid the state of stress is define by an isotropic tensor as

$$T_{ij} = -p\delta_{ij} + T_{ij}^{'} \tag{7}$$

Where, T_{ij} is total stress, $T_{ij}^{'}$ is viscous stress tensor and depends only on the rate of deformation in such a way that the value becomes zero when the fluid is under rigid body motion or rest, p is a scalar whose value is independent explicitly on the rate of deformation and δ_{ij} is kronecker delta. For isotropic linear elastic material, the most general form of $T_{ij}^{'}$ is

$$T_{ij}^{'} = \lambda\Delta\delta_{ij} + 2\mu D_{ij} \tag{8}$$

Where, μ and λ are two material constants. μ is known as first coefficient of viscosity or viscosity and $(\lambda+2\mu/3)$ is second coefficient of viscosity or bulk viscosity. D_{ij} is rate of deformation tensor.

$$D_{ij} = \frac{1}{2}\left(\frac{\partial v_i}{\partial y_j} + \frac{\partial v_j}{\partial x_i}\right) \quad and \quad \Delta = D_{11} + D_{22} + D_{33} \tag{9}$$

Thus, the total stress tensor becomes

$$T_{ij} = -p\delta_{ij} + \lambda\Delta\delta_{ij} + 2\mu D_{ij} \tag{10}$$

For compressible fluid, bulk viscosity $(\lambda+2\mu/3)$ is zero. Thus, the Eq. (10) becomes

$$T_{ij}=-p\delta_{ij}-\frac{2\mu}{3}\Delta\delta_{ij}+2\mu D_{ij} \tag{11a}$$

In case of water like fluid, the viscosity of fluid is neglected, as it is very less in magnitude and the Eq. (5) becomes

$$T_{ij}=-p\delta_{ij} \tag{11b}$$

Generalized Navier-Stokes equations of motion are given by

$$\rho\left(\frac{\partial v_i}{\partial t} + v_j\frac{\partial v_i}{\partial x_j}\right) = \frac{\partial T_{ij}}{\partial x_j} + \rho B \tag{12}$$

Where, B_i is the body force and ρ is density of fluid. Substituting eq. (11-b) in eq. (12) the following relations are obtained.

$$\rho\left(\frac{\partial v_i}{\partial t} + v_j\frac{\partial v_i}{\partial x_j}\right) = \rho B_i - \frac{\partial p}{\partial x_i} \tag{13}$$

If u and v are the velocity components along x and y axes respectively and f_x *and* f_y are body forces along x and y direction respectively, the equation of motion may be written as

$$\frac{1}{\rho}\left(\frac{\partial p}{\partial x} + \frac{\partial u}{\partial t} + u\frac{\partial u}{\partial x} + v\frac{\partial u}{\partial y}\right) = f_x \tag{14}$$

$$\frac{1}{\rho}\left(\frac{\partial p}{\partial y}+\frac{\partial v}{\partial t}+u\frac{\partial v}{\partial x}+v\frac{\partial v}{\partial y}\right)= f_y \tag{15}$$

If body forces are neglected, Eqs. (14) and (15) become

$$\frac{1}{\rho}\left(\frac{\partial p}{\partial x}+\frac{\partial u}{\partial t}+u\frac{\partial u}{\partial x}+v\frac{\partial u}{\partial y}\right)=0 \tag{16}$$

$$\frac{1}{\rho}\left(\frac{\partial p}{\partial y}+\frac{\partial v}{\partial t}+u\frac{\partial v}{\partial x}+v\frac{\partial v}{\partial y}\right)=0 \tag{17}$$

The continuity equation of fluid in two dimensions is expressed as

$$\frac{\partial p}{\partial t}+\rho c^2\left(\frac{\partial u}{\partial x}+\frac{\partial v}{\partial y}\right)=0 \tag{18}$$

Where, c is the acoustic wave speed in fluid. Now, differentiating Eqs. (16) and (17) with respect to x and y respectively, the following relations are obtained.

$$\frac{1}{\rho}\frac{\partial^2 p}{\partial x^2}+\frac{\partial}{\partial x}\left(\frac{\partial u}{\partial t}\right)+\frac{\partial u}{\partial x}\frac{\partial u}{\partial x}+u\frac{\partial^2 u}{\partial x^2}+\frac{\partial u}{\partial y}\frac{\partial v}{\partial x}+v\frac{\partial^2 u}{\partial x\partial y})=0 \tag{19}$$

$$\frac{1}{\rho}\frac{\partial^2 p}{\partial y^2}+\frac{\partial}{\partial y}\left(\frac{\partial v}{\partial t}\right)+\frac{\partial v}{\partial y}\frac{\partial v}{\partial y}+v\frac{\partial^2 v}{\partial y^2}+\frac{\partial u}{\partial y}\frac{\partial v}{\partial x}+u\frac{\partial^2 v}{\partial x\partial y})=0 \tag{20}$$

Adding Eqs. (19) and (20), the following expression is arrived.

$$\begin{aligned}&\frac{1}{\rho}\frac{\partial^2 p}{\partial x^2}+\frac{1}{\rho}\frac{\partial^2 p}{\partial y^2}+\frac{\partial}{\partial x}\left(\frac{\partial u}{\partial t}\right)+\frac{\partial}{\partial y}\left(\frac{\partial v}{\partial t}\right)+\frac{\partial u}{\partial x}\frac{\partial u}{\partial x}+\frac{\partial v}{\partial y}\frac{\partial v}{\partial y}\\&+u\frac{\partial^2 u}{\partial x^2}+v\frac{\partial^2 v}{\partial y^2}+\frac{\partial u}{\partial y}\frac{\partial v}{\partial x}+\frac{\partial u}{\partial y}\frac{\partial v}{\partial x}+v\frac{\partial^2 u}{\partial x\partial y}+u\frac{\partial^2 u}{\partial x\partial y})=0\end{aligned} \tag{21}$$

Differentiating Eq. (18) with respect to time, the following expression can be obtained.

$$\frac{\partial^2 p}{\partial t^2}+\rho c^2\left\{\frac{\partial}{\partial x}\left(\frac{\partial u}{\partial t}\right)+\frac{\partial}{\partial y}\left(\frac{\partial v}{\partial t}\right)\right\}=0 \tag{22}$$

Thus, from Eqs. (21) and (22), one can find the following expression

$$\begin{aligned}&\frac{1}{\rho}\frac{\partial^2 p}{\partial x^2}+\frac{1}{\rho}\frac{\partial^2 p}{\partial y^2}-\frac{1}{\rho c^2}\frac{\partial^2 p}{\partial t^2}+\frac{\partial u}{\partial x}\frac{\partial u}{\partial x}+\frac{\partial v}{\partial y}\frac{\partial v}{\partial y}+u\frac{\partial^2 u}{\partial x^2}+v\frac{\partial^2 v}{\partial y^2}+\frac{\partial u}{\partial y}\frac{\partial v}{\partial x}+\\&\frac{\partial u}{\partial y}\frac{\partial v}{\partial x}+v\frac{\partial^2 u}{\partial x\partial y}+u\frac{\partial^2 u}{\partial x\partial y})=0\end{aligned} \tag{23}$$

Neglecting higher order terms in Eq. (23), the equation becomes

$$\frac{1}{\rho}\frac{\partial^2 p}{\partial x^2}+\frac{1}{\rho}\frac{\partial^2 p}{\partial y^2}-\frac{1}{\rho c^2}\frac{\partial^2 p}{\partial t^2}+\frac{\partial u}{\partial x}\frac{\partial u}{\partial x}+\frac{\partial v}{\partial y}\frac{\partial v}{\partial y}+\frac{\partial u}{\partial y}\frac{\partial v}{\partial x}+\frac{\partial u}{\partial y}\frac{\partial v}{\partial x}=0 \tag{24}$$

In the present study, the water is considered to be linearly compressible with very small amount of irrotational movement (Kassiotis *et al*. 2010, 2011a, b). Hence, the Eq. (24) becomes

$$\frac{1}{\rho}\frac{\partial^2 p}{\partial x^2}+\frac{1}{\rho}\frac{\partial^2 p}{\partial y^2}=\frac{1}{\rho c^2}\frac{\partial^2 p}{\partial t^2} \tag{25}$$

The pressure distribution in the fluid domain may be obtained by solving Eq. (25) with the following boundary conditions. A typical geometry of tank-water system is shown in Fig. 1.

(i) At surface I

Considering the effect of surface wave of the fluid, the boundary condition of the free surface is taken as

$$\frac{1}{g}\ddot{p}+\frac{\partial p}{\partial y}=0 \tag{26}$$

(ii) At surface II

This surface is considered as rigid surface and thus pressure should satisfy the following condition

$$\frac{\partial p}{\partial n}\left(x,0,t\right)=0.0 \tag{27}$$

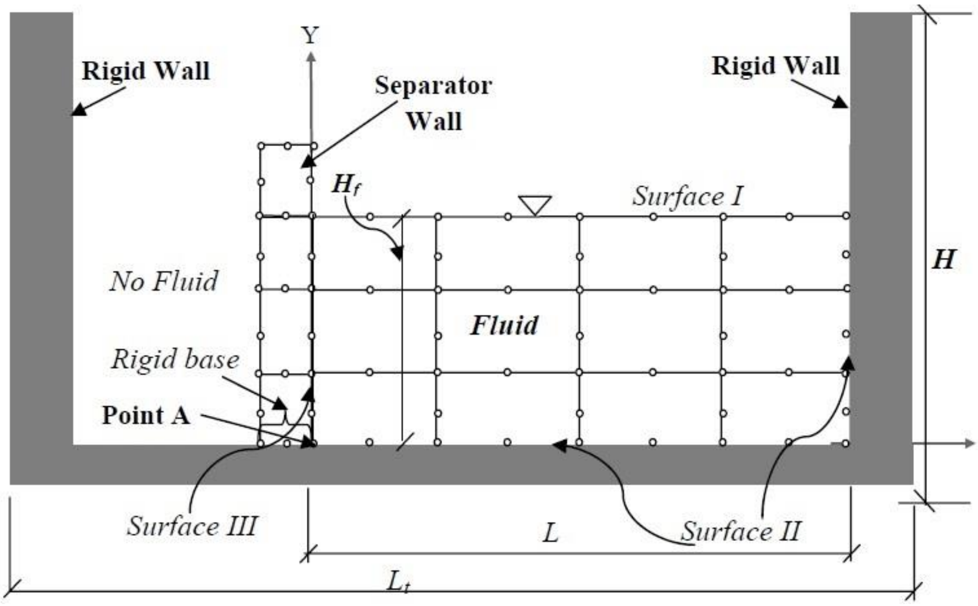

Fig. 1 A typical finite element discretization of tank-water system

(iii) At surface III

At water-tank wall interface, the pressure should satisfy

$$\frac{\partial p}{\partial n}(0, y, t) = \rho_f a e^{i\omega t} \tag{28}$$

Where $ae^{i\omega t}$ is the horizontal component of the ground acceleration in which, ω is the circular frequency of vibration and $i = \sqrt{-1}$,n is the outwardly directed normal to the element surface along the interface. ρ_f is the mass density of the fluid.

2.2.1 Finite element formulation for fluid domain

By Galerkin approach and assuming pressure to be the nodal unknown variable, the discretised form of Eq. (25) may be written as

$$\int_{\Omega} N_r \left[\frac{1}{\rho} \frac{\partial^2 p}{\partial x^2} + \frac{1}{\rho} \frac{\partial^2 p}{\partial y^2} - \frac{1}{\rho c^2} \left(\frac{\partial^2 p}{\partial t^2} \right) \right] d\Omega = 0 \tag{29}$$

Where, N_r is the interpolation function for the fluid and Ω is the region under consideration. Using Green's theorem Eq. (29) may be transformed to

$$\frac{1}{\rho} \int_{\Gamma} N_r \left(\frac{\partial p}{\partial x} + \frac{\partial p}{\partial y} \right) d\Gamma - \int_{\Gamma} \left(\frac{\partial N_r}{\partial x} \frac{\partial p}{\partial x} + \frac{\partial N_r}{\partial y} \frac{\partial p}{\partial y} \right) d\Gamma - \frac{1}{\rho c^2} \int_{\Gamma} \frac{\partial^2 p}{\partial t^2} d\Gamma \tag{30}$$

The first term of the above equation may be written as

$$\frac{1}{\rho} \int_{\Gamma} N_r \left(\frac{\partial p}{\partial x} + \frac{\partial p}{\partial y} \right) d\Gamma - \int_{\Gamma} \left(\frac{\partial N_r}{\partial x} \frac{\partial p}{\partial x} + \frac{\partial N_r}{\partial y} \frac{\partial p}{\partial y} \right) d\Gamma - \frac{1}{\rho c^2} \int_{\Gamma} \frac{\partial^2 p}{\partial t^2} d\Gamma \tag{31}$$

The whole system of Eq. (30) may be written in a matrix form as

$$[\overline{H}]\{\ddot{p}\} + [\overline{G}]\{p\} = \{B\} \tag{32}$$

in which

$$\left.\begin{aligned} [\overline{H}] &= \frac{1}{c^2} \sum \int_{\Gamma} [N_r]^T [N_r] d\Gamma \\ [\overline{G}] &= \sum \int_{\Gamma} \left[\frac{\partial}{\partial x}[N_r]^T \frac{\partial}{\partial x}[N_r] + \frac{\partial}{\partial y}[N_r]^T \frac{\partial}{\partial y}[N_r] \right] d\Gamma \\ \{\mathbf{B}\} &= \sum \int [N_r]^T \frac{\partial p}{\partial x} d\Gamma = B_1 + B_2 + B_3 \end{aligned}\right\} \tag{33}$$

According to the boundary conditions for the fluid domain, if linearised surface wave condition is adopted (Eq. (26)), the same may be written in finite element form as

$$\{B_I\} = -\frac{1}{g}[R_I]\{\ddot{p}\} \tag{34}$$

in which

$$\left[R_I\right]=\sum\int_{\Gamma_I}\left[N_r\right]^T\left[N_r\right]d\Gamma \tag{35}$$

At the *surface II* (Eq. (27))

$$\{B_{II}\}=0 \tag{36}$$

At the *surface III* (Eq. (28)), if $\{a\}$ is the vector of nodal accelerations of generalized coordinates, $\{B_{III}\}$ may be expressed as

$$\{\mathbf{B}_{III}\}=\rho R_{III}\,a \tag{37}$$

where

$$\{R_{III}\}=\sum\int_{\Gamma_{III}}[N_r]^T[T][N_r]d\Gamma \tag{38}$$

Here, *[T]* is the transformation matrix for generalized accelerations of a point on the fluid structure interface and $[N_d]$ is the matrix of shape functions of the tank wall.

Substitution of all terms in Eq. (32) gives

$$[H]\{\ddot{p}\}+[A]\{\dot{p}\}+[G]\{p\}=\{F_r\} \tag{39}$$

Here, $[H]$, $[A]$, $[G]$ and $\{F_r\}$ can be expressed as

$$\left.\begin{aligned}\left[H\right]&=\left[\bar{H}\right]+\frac{1}{g}\left[R_I\right]\\ \left[A\right]&=[0]\\ \left[G\right]&=\left[\bar{G}\right]\\ \{F_r\}&=\rho([R_{III}]\{a\})\end{aligned}\right\} \tag{40}$$

For any prescribed acceleration at the dam-reservoir interface and reservoir bed interface, Eq. (39) is solved to obtain the hydrodynamic pressure in the reservoir.

2.3 Direct coupling for fluid-structure system

In the fluid-structure interaction problems, the structure and the fluid do not vibrate as separate systems under external excitations, rather they act together in a coupled way. Therefore, this fluid-structure interaction problem has to be dealt in a coupled way. In present study, a strong coupling approach is developed to get the coupled water-separator wall response under external excitation. The coupling of structure and fluid may be formulated in following way.

The discrete structural equation with damping may be written as

$$M\ddot{u}+C\dot{u}+Ku-Qp-F_d=0 \tag{41}$$

The coupling term *[Q]* in Eq. (41) arises due to the acceleration and pressure specified on the water-separator wall interface boundary (Zienkiewicz and Newton 1969) and can be expressed as

$$\int_{\Gamma_s} N_s^T n p d\Gamma = \left(\int_{\Gamma_s} N_s^T n N_r d\Gamma \right) p = Qp \tag{42}$$

Where, n is the direction vector of the normal to the water-separator wall interface. N_s and N_r are the shape functions of separator wall and water respectively. Similarly, discretized fluid equation may be written as

$$E\ddot{p} + A\dot{p} + Gp + Q^T \ddot{u} - F_r = 0 \tag{43}$$

Now, the system of Eqs. (41) and (43) are coupled in a second-order ordinary differential equations, which defines the coupled water-separator wall system completely. The Eqs. (41) and (43) may be written as a set

$$\begin{bmatrix} M & 0 \\ Q^T & E \end{bmatrix} \begin{Bmatrix} \ddot{u} \\ \ddot{p} \end{Bmatrix} + \begin{bmatrix} C & 0 \\ 0 & A \end{bmatrix} \begin{Bmatrix} \dot{u} \\ \dot{p} \end{Bmatrix} + \begin{bmatrix} K & -Q \\ 0 & G \end{bmatrix} \begin{Bmatrix} u \\ p \end{Bmatrix} = \begin{Bmatrix} F_d \\ F_r \end{Bmatrix} \tag{44}$$

For free vibrations analysis, the above equation can be simplified to the following expression after omitting all the damping terms

$$\begin{bmatrix} M & 0 \\ Q^T & E \end{bmatrix} \begin{Bmatrix} \ddot{u} \\ \ddot{p} \end{Bmatrix} + \begin{bmatrix} K & -Q \\ 0 & G \end{bmatrix} \begin{Bmatrix} u \\ p \end{Bmatrix} = 0 \tag{45}$$

Natural frequency of water-separator wall system can be obtained by eigenvalue solution of Eq. (45). However, the matrices in Eq. (37) are unsymmetrical and standard eigenvalue solutions cannot be used directly. So the above matrices are to be transformed into symmetric matrices. This can be accomplished by change of variables as follows. Introducing two variables $\tilde{u} = ue^{i\omega t}$ and $\tilde{p} = pe^{i\omega t}$, Eq. (45) can be expressed as

$$K\tilde{u} - Q\tilde{p} - \omega^2 M\tilde{u} \tag{46}$$

$$E\tilde{p} - \omega^2 Q^T \tilde{u} - \omega^2 G\tilde{p} \tag{47}$$

Further, introducing another variable q such that

$$\tilde{p} = \omega^2 q \tag{48}$$

After manipulation and substitution of above three equations in eq. (45), the final form of this equation becomes

$$\left[\begin{bmatrix} K & 0 & 0 \\ 0 & A & 0 \\ 0 & 0 & 0 \end{bmatrix} - \omega^2 \begin{bmatrix} M & 0 & Q \\ 0 & 0 & E \\ Q^T & E^T & G \end{bmatrix} \right] \begin{Bmatrix} \tilde{u} \\ \tilde{p} \\ \tilde{q} \end{Bmatrix} = 0 \tag{49}$$

The above matrices in fluid-structure system are symmetric and are in standard form. Further, the variable can be eliminated by static condensation and the final water-separator wall system becomes symmetric and still contains only the basic variables.

2.4 Indirect coupling for fluid-structure system

The coupled effect of fluid-structure system can also be achieved by an iterative scheme. At any time instant *t*, hydrodynamic pressure in water is evaluated by solving Eq. (39) with appropriate boundary conditions and considering the structure to be rigid. But, the result is inaccurate because in practical, the separator wall is elastic in nature. To determine accurate hydrodynamic pressure, forces developed due to hydrodynamic pressures at rigid water-separator wall interface are considered as additional forces on the adjacent separator. Hence, at the same time instant, the structure is analyzed with these additional forces $\{F_{rr}\}$, using Eq. (50).

$$M\ddot{u} + C\dot{u} + Ku = -F_d - F_{rr} \tag{50}$$

Here, the external force F_d can be expressed as follows.

$$F_d = M\ddot{u}_g \tag{51}$$

The ground acceleration is considered as $\ddot{u}_g$. Due to these additional forces, the separator wall undergoes a displacement $\{d\}_t$, as a result boundary condition at the water-separator wall interface changes. Therefore, the water domain is solved again with the changed displacement at water-separator wall interface. Thus at time *t*, both the hydrodynamic pressure $\{p\}_t$ and the structural displacement $\{d\}_t$ are iterated simultaneously till a desired level of convergence is achieved (Maity and Bhattacharyy 2003). Thus

$$\left|\frac{\{p_{i+1}\}_t - \{p_i\}_t}{\{p_i\}_t}\right| \leq \varepsilon', \text{ and } \left|\frac{\{d_{i+1}\}_t - \{d_i\}_t}{\{d_i\}_t}\right| \leq \varepsilon'' \tag{52}$$

Where, *i* is the no. of iteration. ε' and ε'' are small pre-assigned tolerance values. For an efficient and accurate analysis of water-separator wall coupled system, the steps to be followed are given in the form of flow chart in Fig. 2.

2.5 Computation of velocity and displacement of fluid

The accelerations of the fluid particles can be calculated after computing the hydrodynamic pressure in the water tank. The velocity of the fluid particle may be calculated from the known values of acceleration at any instant of time using Gill's time integration scheme (Gill 1951) which is a step-by-step integration procedure based on Runge-Kutta method (Ralston and Wilf 1965). This procedure is advantageous over other available methods as it (i) needs less storage registers, (ii) controls the growth of rounding errors,(iii) is usually stable and (iv) is computationally economical. At any instant of time *t*, velocity will be

$$V_t = V_{t-\Delta t} + \Delta t V_t \tag{53}$$

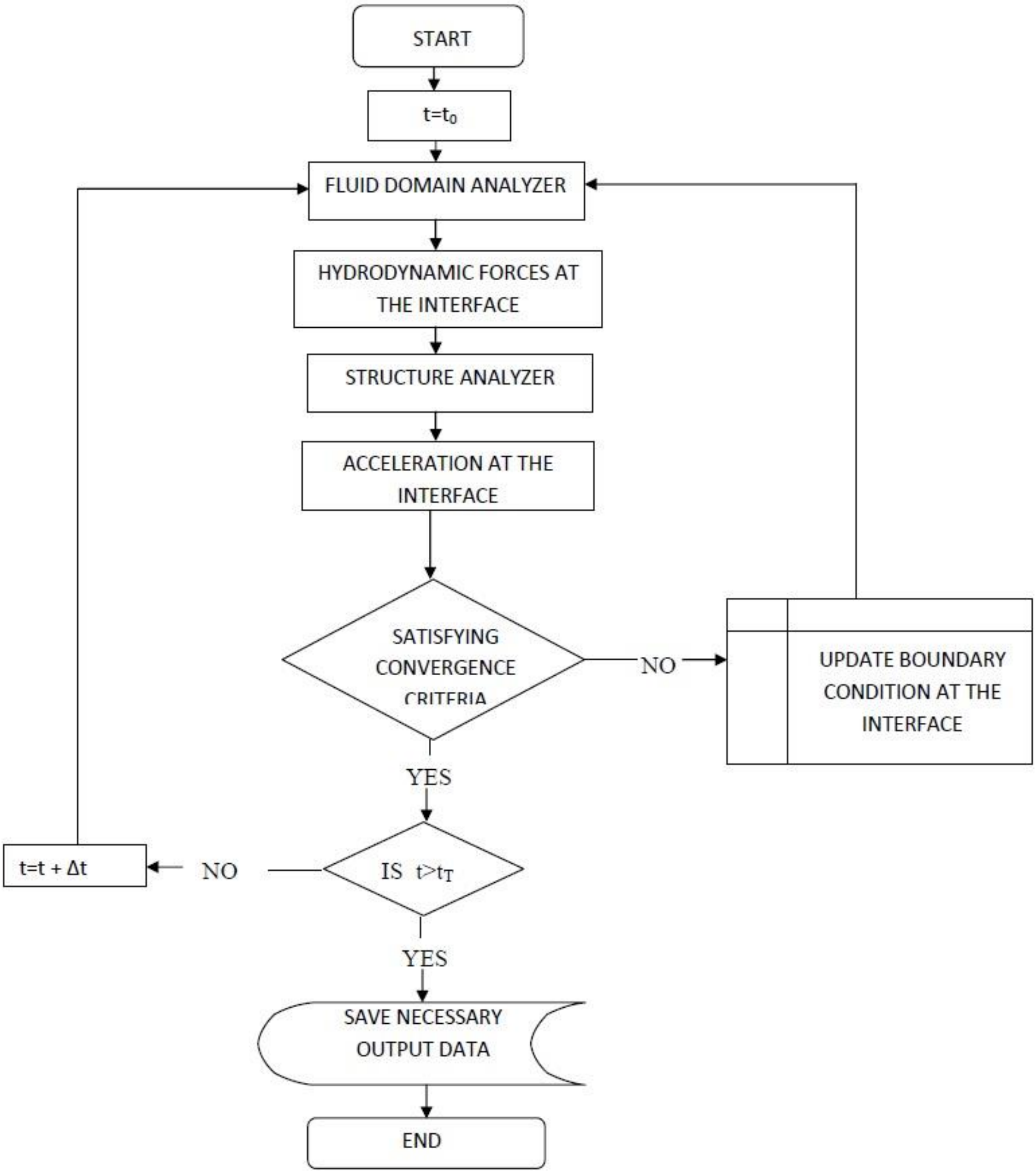

Fig. 2 One of the PLVM of the undamaged structure

Velocity vectors in the fluid domain may be plotted based on velocities computed at the Gauss points of each individual element and then extrapolating to their nodal points. Similarly, the displacement of fluid particles in the fluid domain, U at every time instant can also be computed as

$$U_t = U_{t-\Delta t} + \Delta t U_t \tag{54}$$

3. Numerical results

Example 1: Validation of direct coupling

The accuracy of the proposed strong coupled approach is studied considering a bench marked problem. The results are compared with an existing literature (Sami and Lotfi 2007) for the Pine flat dam. The material properties of dam and reservoir are considered as follows: modulus of elasticity=22.75GPa,Poisson's ratio=0.2, unit weight of concrete=2480 kg/m^3, pressure wave velocity = 1440 m/s, unit weight of water = 981kg/m^3,height of dam (H_d) = 121.91 m, width at top (t_d) = 9.75 m, width at base (L_d) = 95.71,depth of reservoir (H_f)= 116.19 m. Fig. 3 shows the geometric details and a typical finite element discretization for the dam-reservoir system. For the finite element analysis, the infinite reservoir is truncated at a distance (L_t) 200 m from dam-reservoir interface and Somerfeld's boundary condition is implemented at truncation surface as considered by Sami and Lotfi (2007). The first five natural frequencies of the dam-reservoir system are listed and compared with those values obtained by Samii and Lotfi (2007) in Table 1. The tabulated results show the accuracy of the developed direct coupled approach.

Example 2: Efficiency of direct coupling

In order to investigate the efficiency of direct coupling, a comparative study with indirect coupling is carried out with the following geometric and material properties of water-separator wall system. Size of tank = 56 m × 20 m (L_t) × 15 m (H), height of separator wall (H_s) = 12.5 m, modulus of elasticity = 200 GPa, Poison's ratio = 0.3, structural damping = 5 %, depth of fluid (H_f) = 10 m, mass density of fluid = 1000 kg/m^3, mass density of separator wall = 7800 kg/m^3. Here the flexible separator wall and water domain are discretized by 2 × 10 (i.e., N_h = 2 and N_v = 10) and 10 ×8 (i.e., N_h = 10 and N_v = 8) respectively. A typical finite element discretization of water-separator wall system is shown in Fig. 1.

Table 1 First five natural frequencies of the Pine flat dam-reservoir system

Mode number	Natural Frequency (Hz)	
	Present Study	Samii and Lotfi [12]
1	2.5341	2.5267
2	3.2712	3.2681
3	4.5626	4.6651
4	6.2326	6.2126
5	7.9435	7.9181

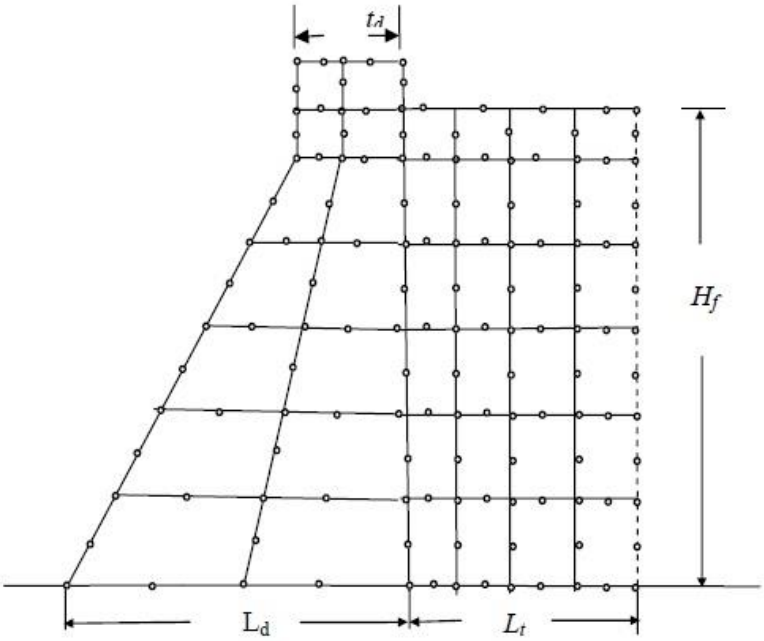

Fig. 3 Finite element mesh of dam-reservoir system

The comparative study is carried out for L= 10 m and the responses of water-separator wall system are determined due to the ramp acceleration of unit amplitude. For indirect method, the tolerance value is considered as 10^{-3} because for this value the responses of water-separator wall system converged sufficiently. The displacement of flexible separator wall and hydrodynamic pressure at the point A (Fig. A) determined from different coupling methods are presented in Fig. 4 and Fig. 5 respectively. The tip displacements from both the methods follow the similar pattern. However, the pattern obtained from indirect method is shifted toward right, when it is compared to the pattern from direct method. The Fig. 4 also depicts that the displacement values obtained from the indirect method is larger than those obtained from direct method. This difference becomes larger, when the hydrodynamic pressure at the point A (Fig. 1) is compared (Fig. 5). In case of direct coupling, the separator wall and the water vibrate as a single system and the natural frequency of it is the coupled natural frequency of separator wall-water system. However, in indirect coupling separator wall and water vibrate separately and their natural frequencies are higher than the natural frequency obtained from direct coupling approach i.e., coupled natural frequency of separator wall-water system. This is the main reason for obtaining different values in Figs. 4 and 5. The CPU time for these two methods is listed in Table 2. The computer program have been run in a PC of following configuration: Processor:- Intel(R) Core(TM) 2 Duo CPU T5870 @ 2.00 GHz, Installed memory (RAM):- 3.00 GHz, System type:- 32 bit operating system. The comparison of CPU times in Table 2 shows that the CPU time for direct coupling is quite less with that for indirect coupling. Therefore, direct coupling method is considered as most suitable method of analysis of fluid-structure interaction problems and it is used in further analysis of water-separator wall system in present analysis.

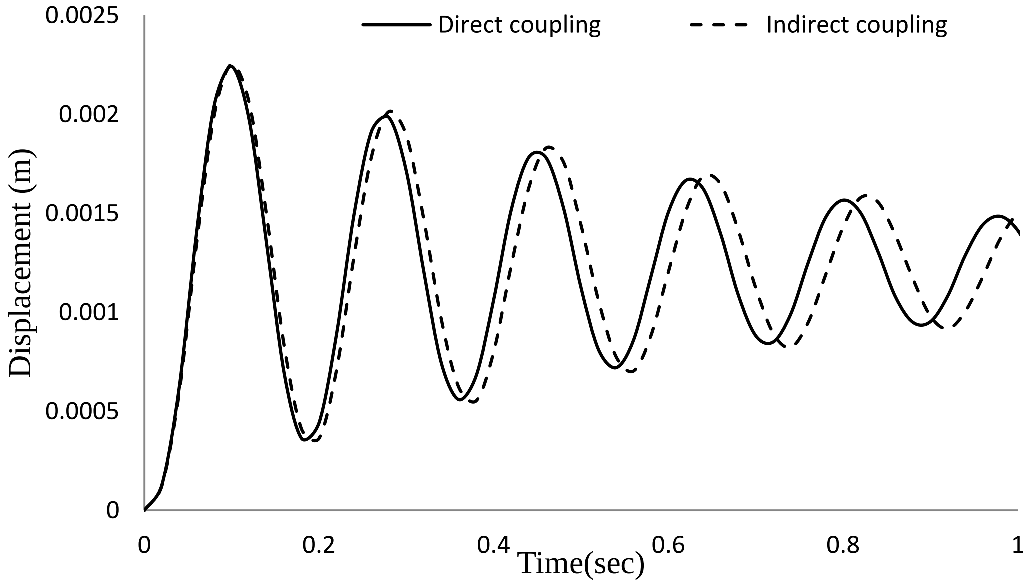

Fig. 4 Tip displacement of the separator wall due to ramp acceleration

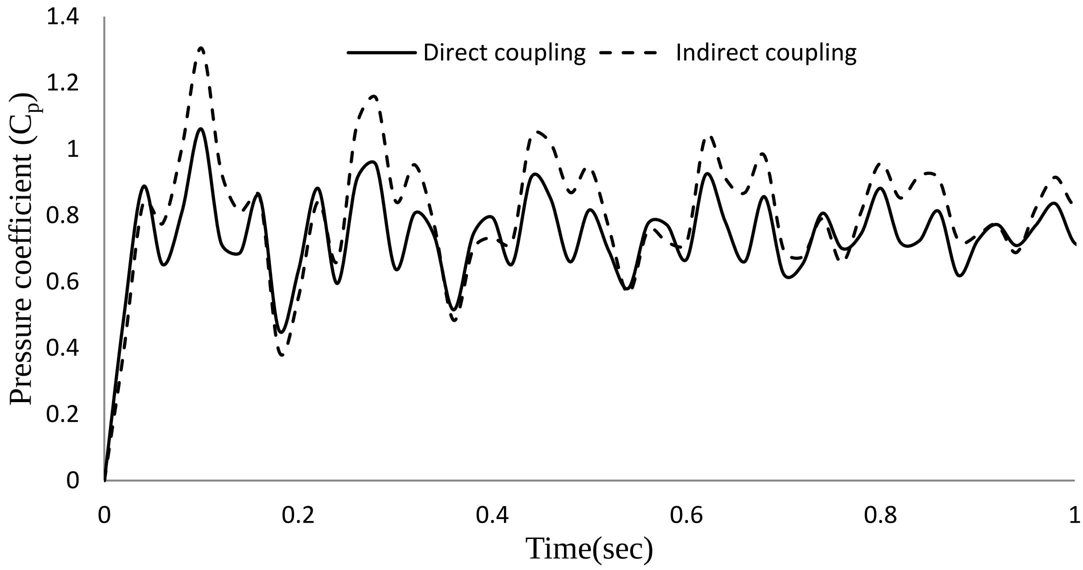

Fig. 5 Hydrodynamic pressure at point A due to ramp acceleration

Table 2 CPU time for analysis of dam-reservoir system

CPU time (sec)	
Direct coupling	Indirect coupling
115	865

Example 3: Responses of tank due earthquake excitation

Geometric and material properties considered in this case are same as considered in example 2 except the length of tank. The performance of water-separator wall system is studied for two different tank lengths, i.e., 5 m and 15 m and discretized by 2 × 8 (i.e., N_h = 2 and N_v = 8), 10 × 8 (i.e., N_h = 10 and N_v = 8) respectively. The study is carried out due to the horizontal component of Koyna earthquake (Fig. 6). Displacement at the tip of the separator wall for different tank length is compared in Fig. 7. The figure shows the incremental trend with the decrease of the tank length. However, this increase is not so prominent. Similar observation is obtained while the major principal stresses at the base of the separator for different length of the tank are compared (Fig. 8). The hydrodynamic pressure at point A is also presented in Fig. 9. In this case, the hydrodynamic pressure for tank length of 5.0 m is almost two times of the hydrodynamic pressure for tank length of 10 m. These two observations imply that the behavior of the water in the tank may be altered by the lengths of the tank. However, the length of the tank does not have so much effect on the performance of separator wall.

Hydrodynamic pressure along the face of the separator wall for tank of length 5 m and 15 m are shown in Fig. 10 and Fig. 11 respectively and the pressure is compared with the corresponding pressure for rigid wall. The maximum pressure on the elastic walls is almost equal to maximum hydrodynamic pressure corresponding rigid for tank length of 15 m. For tank of length 5 m, maximum hydrodynamic pressure on flexible separator wall is lower than that for rigid wall. However, the distributions of hydrodynamic pressure for flexible and rigid wall for both the length of the tank are of quite different natures. The maximum hydrodynamic pressure for flexible separator wall no longer occurs at the base of the wall as in the rigid case, but shifts upwards to a distance near about $2H_f/3$ and $H_f/2$ above the base for tank length of 15 m and 5 m respectively. The upward shifting of the peak hydrodynamic pressure implies that the bending moment exerted by the hydrodynamic loading is larger than that predicted by the rigid wall analysis.

Fig. 12 shows the sloshed displacement for different lengths of the water tank. Horizontal axis of the figure shows a dimension less parameter (x/L). The sloshed displacement for tank length of 5 m is comparatively higher than that of tank of 15 m length. For deep water case i.e., H_f =10 m and L= 5 m, the tank wall affect the responses of separator wall significantly. For comparatively lower tank length, the sloshed displacement of the free surface becomes very large and it enhances the hydrodynamic pressure within the water domain. The velocity vectors in the fluid domain are plotted in Fig. 12. The vertical axis represents the height of the water and the horizontal axis represents the length between elastic separator wall and rigid tank wall. Figs. 13 (a) and 13 (b) clearly show that the fluid generates a tendency to rotate. However, this rotating tendency is more in case of lower tank length and this rotating tendency increases the hydrodynamic pressure in fluid domain.

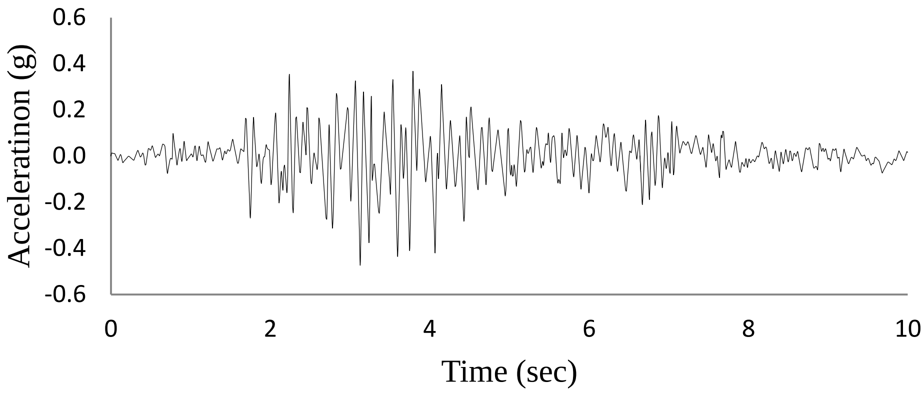

Fig. 6 Horizontal component of Koyna earthquake

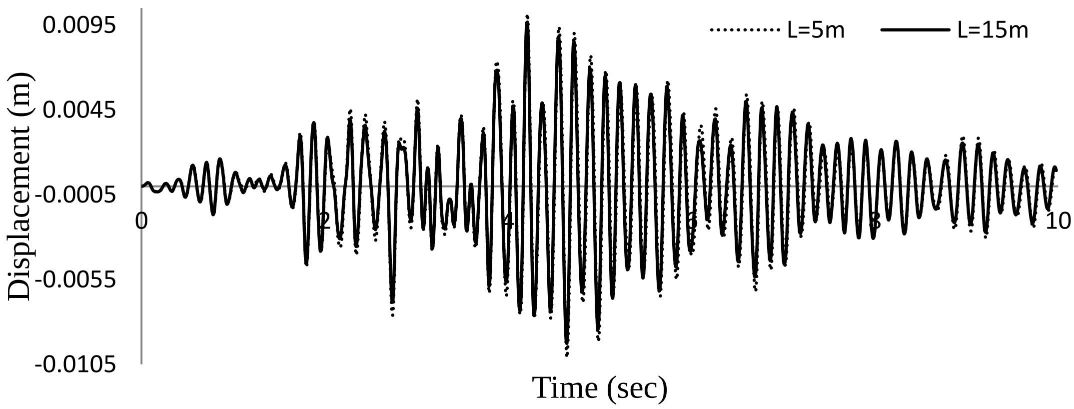

Fig. 7 Tip displacement of separator wall due to Koyna earthquake

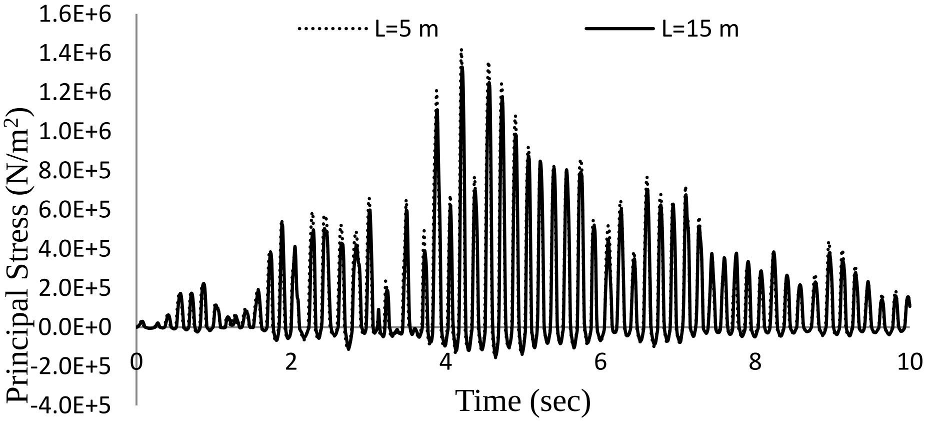

Fig. 8 Major Principal stress at the base of the separator wall due to Koyna earthquake

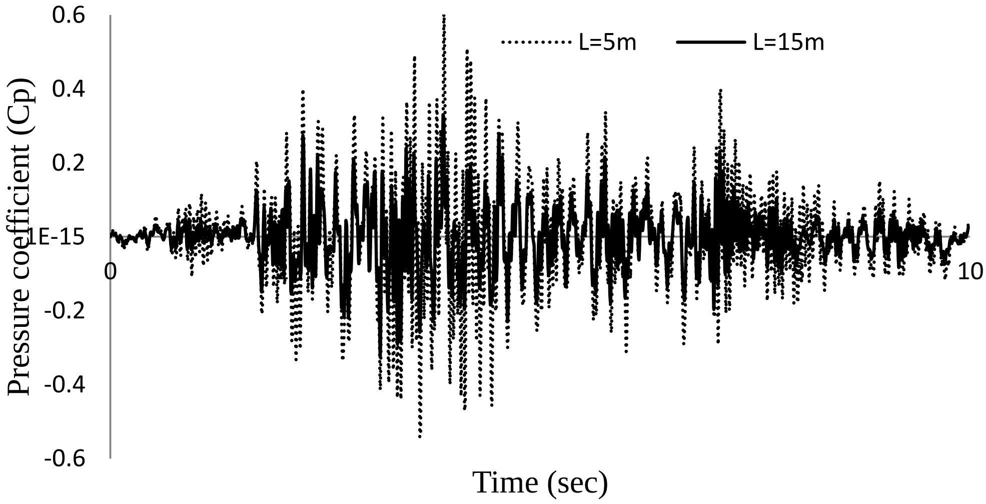

Fig. 9 Hydrodynamic pressure at point A due to Koyna earthquake

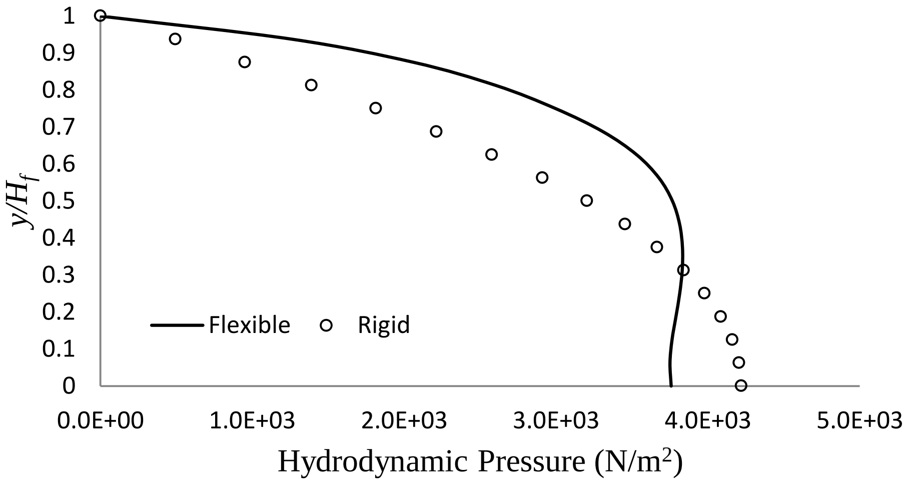

Fig. 10 Hydrodynamic pressure along the separator wall at t= 4.20 sec for L=5 m

4. Conclusions

This paper presents a pressure based finite element analysis of water tank with elastic separator wall. This pressure formulation of fluid domain has certain advantages in the computational aspect compared to the velocity potential and the displacement-based formulations, as the number of independent variable per node is only one. A direct formulation is used to couple the fluid and elastic separator wall. From some typical numerical problem solved in the present study it is observed that the coupling phenomena are found to have great significance in the case of fluid-structure interaction analysis.

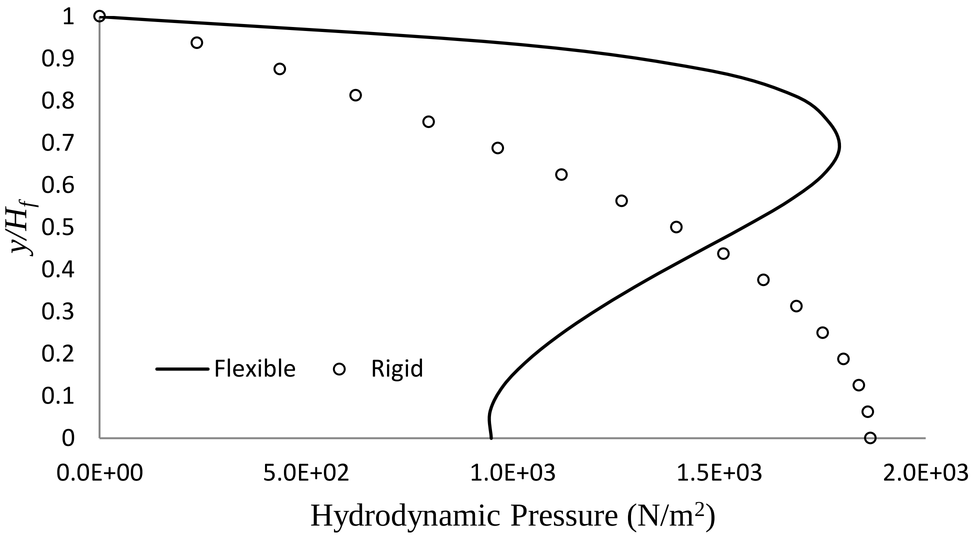

Fig. 11 Hydrodynamic pressure along the separator wall at t = 4.20 sec for L=15 m

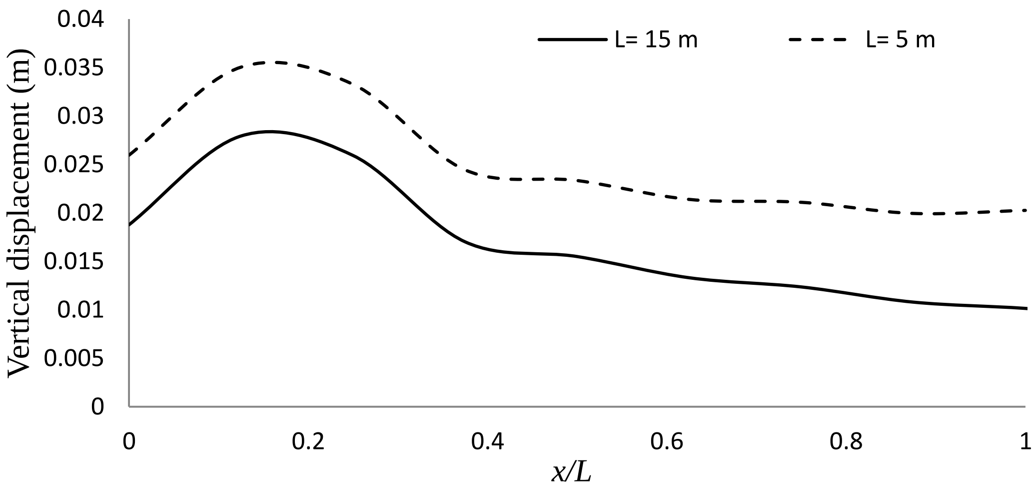

Fig. 12 Sloshed displacement for different length of tank at t= 4.20 sec

The hydrodynamic pressure is reduced if the elastic effect of separator is taken into consideration. The hydrodynamic pressure is increased for comparatively lower tank length. The displacement at the free surface of the tank is comparatively higher for lower tank length. The rotating tendency of fluid is more when the distance between the tank wall and elastic separator is less. These two critical observations are the main reason to obtain comparatively higher hydrodynamic pressure for lower tank length.

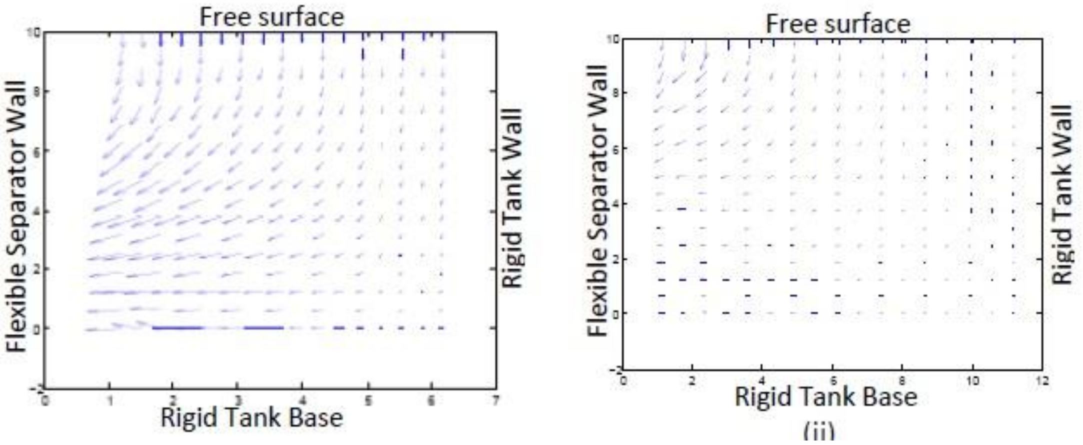

(a) (b)

Fig. 13 Velocity vectors at t = 4.20 sec in fluid for (a) L =5 m and (b) L =15 m

References

Akkose, M., Adanur, S., Bayraktar, A. and Dumanoglu, A.A. (2008), “Elasto-plastic earthquake response of arch dams including fluid–structure interaction by the Lagrangian approach”, *Appl. Math. Model.*, **32**(11), 2396-2412.

Antoniadis, I. and Kanarachos, A. (1998), “Decoupling procedures for fluid-structure interaction problems”, *Comput. Method. Appl. M.*, **70**(1), 1-25.

Barrios, H. H., Zavoni, E.H., Alvaro, A. and Rodriguez, A. (2007), “Nonlinear sloshing response of cylindrical tanks subjected to earthquake ground motion”, *Eng. Struct.*, **29**(12), 3364-3376.

Bermudez, A., Duran, R., Muschietti, M.A., Rodriguez, R. and Solomin, J. (1995), “Finite element vibration analysis of fluid–solid systems without spurious modes”, *SIAM J. Numer. Anal.*, **32**(4), 1280-1295.

Biswal, K.C., Bhattacharyya, S.K. and Sinha. P.K. (2006), “Non-linear sloshing in partially liquid filled containers with baffles”, *Int. J. Numer. Meth. Eng.*, **68**(3), 317-337

Bouaanani, N. and Lu. F.Y. (2009), “Assessment of potential-based fluid finite elements for seismic analysis of dam–reservoir systems”, *Comput. Struct.*, **87**(3-4), 206-224.

Chen, H.C. and Taylor, R.L. (1990), “Vibration analysis of fluid solid systems using a finite element displacement formulation”, *Int. J. Numer. Method. Eng.*, **29**(4), 683-698.

Chopra, A.K. (1967), “Hydrodynamic pressures on dams during earthquakes”, *J. Eng. Mech. - ASCE*, **93**(6), 205-223.

Choun, Y.S. and Yun, C.B. (1996), “Sloshing characteristic in rectangular tanks with a submerged block”, *Comput. Struct.*, **61**(3), 401-413.

Chwang, A.T. (1978), “Hydrodynamic pressure on sloping dams during earthquakes. Part - 2.Exact theory”, *J. Fluid Mech.*, **87**(2), 343-348.

Gill, S. (1951), “A process for the step-by-step integration of differential equations in an automatic digital computing machine”, *Proceedings of the Cambridge Philosophical Society*, **47**(1), 96-108.

Gogoi, I. and Maity, D. (2005), “Seismic safety of aged concrete gravity dams considering fluid-structure interaction”, *J. Earthq. Eng.*, **9**(5), 1-20.

Hua, C.W., Fuh, C.B. and Kan. H.T. (2013), “Hydrodynamic forces induced by transient sloshing in a 3D rectangular tank due to oblique horizontal excitation”, *J. Comput. Math. Appl.*, **65**(8), 1163-1186.

Kassiotis, C., Ibrahimbegovic, A. and Matthies, H. (2010), “Partitioned solution to fluid-structure interaction

problem in application to free-surface flow", *Eur. J. Mech. Part B: Fluids*, **29**(6), 510-521.
Kassiotis, C., Ibrahimbegovic, A., Niekamp, R. and Matthies, H. (2011a), "Partitioned solution to nonlinear fluid-structure interaction problems. Part I: implicit coupling algorithms and stability proof", *Comput. Mech.*, **47**, 305-323.
Kassiotis, C., Ibrahimbegovic, A., Niekamp, R. and Matthies, H. (2011b), "Partitioned solution to nonlinear fluid-structure interaction problems. Part II: CTL based software implementation with nested parallelization", *Comput. Mech.*, **47**, 335-357.
Lotfi, V. (2004), "Frequency domain analysis of concrete gravity dams by decoupled modal approach", *Dam Eng.*, **15**(2), 141-165.
Maity, D. and Bhattacharyya, S.K. **(**1997), "Finite element analysis of fluid-structure system for small fluid displacement", *Int. J. Struct.*, **17**, 1-18**.**
Maity, D. and Bhattacharyya, S.K. (2003), "A parametric study on fluid-structure interaction problems", *J. Sound Vib*., **263**(4), 917-935.
Olson, L.G. and Bathe, K.J. (1983), "A study of displacement-based fluid finite elements for calculating frequencies of fluid and fluid–structure systems", *Nuclear Eng. Des.*, **76**(2), 137-151.
Onate, E., Garcıa, J., Idelsohn, R. and Delpin, S. (2006), "Finite calculus formulations for finite element analysis of incompressible flows. Eulerian, ALE and Lagrangian approaches", *Comput. Method. Appl. M*., **195**(23-24), 3001-3037.
Pal, P. and Bhattacharyya, S.K. (2013), "Slosh dynamics of liquid-filled composite containers: A two dimensional meshless local Petrov-Galerkin approach", *J. Fluid. Struct*., **39**, 60-75.
Pani, P.K. and Bhattacharyy, S.K. (2007), "Fluid–structure interaction effects on dynamic pressure of a rectangular lock-gate", *J. Finite Elem. Anal. Des.*, **43**(10), 739-748.
Panigrahy, P.K., Saha, U.K. and Maity. D. (2009), "Experimental studies on sloshing behavior due to horizontal movement of liquids in baffled tanks", *J. Ocean Eng*., **36**(3-4), 213-222.
Ralston, A. and Wilf, H.S. (1965), *Mathematical Models for Digital Computers*, Wiley1, New York.
Sami, A. and Lotfi, V. (2007), "Comparison of coupled and decoupled modal approaches in seismic analysis of concrete gravity dams in time domain", *Finite Elem. Anal. Des.*, **43**(13), 1003- 1012.
Singh, R.K., Kant, T. and Kakodkar, A. (1991), "Coupled shell-fluid interaction problems with degenerate shell and three-dimensional fluid elements", *Comput. Struct*., **38**(5-6), 515-528.
Tung, C.C. (1979), "Hydrodynamic forces on submerged vertical circular cylindrical tanks underground excitation", *Appl. Ocean Res*., **1**(2), 75-78.
Williams, A.N. and Moubayed, W.I. (1990), "Earthquake-induced hydrodynamic pressures on submerged cylindrical storage tanks", *J. Ocean Eng.*, **17**(3), 181-199.
Zienkiewicz, O.C. and Newton, R.E. (1969), "Coupled vibration of a structure submerged in a compressible Fluid", *Proceedings of the International Symposium on Finite Element Techniques*, Stuttgart.